

Constraints on the mass and abundance of black holes in the Galactic halo: the high mass limit

Chigurupati Murali¹, Phil Arras² and Ira Wasserman²

¹Canadian Institute for Theoretical Astrophysics, McLennan Labs, University of Toronto, 60 St. George St., Toronto M5S 3H8, Canada

²Center for Radiophysics and Space Research, Cornell University

1 April 2018

ABSTRACT

We establish constraints on the mass and abundance of black holes in the Galactic halo by determining their impact on globular clusters which are conventionally considered to be little evolved. Using detailed Monte Carlo simulations, and simple evolutionary models, we argue that black holes with masses $M_{bh} \gtrsim (1 - 3) \times 10^6 M_\odot$ can comprise no more than a fraction $f_{bh} \approx 0.17$ of the total halo density at Galactocentric radius $R \approx 8$ kpc. This bound arises from requiring stability of the cluster mass function. A more restrictive bound may be derived if we demand that the probability of destruction of any given, low mass ($M_c \approx (2.5 - 7.5) \times 10^4 M_\odot$) globular cluster not exceed 50%; this bound is $f_{bh} \lesssim 0.025 - 0.5$ at $R \approx 8$ kpc. This constraint improves those based on disk heating and dynamical friction arguments as well as current lensing results. At smaller radius, the constraint on f_{bh} strengthens, while, at larger radius, an increased fraction of black holes is allowed.

Key words: globular clusters: general – Galaxy: halo – Galaxy: structure – dark matter

1 INTRODUCTION

What is the form and structure of dark matter in galactic halos? A variety of both baryonic and non-baryonic candidates exist (see Carr 1994 for a review of baryonic dark matter candidates) but there are relatively few constraints so the question remains.

One longstanding suggestion is that of Lacey & Ostriker (1985) who proposed that halo dark matter consists of massive black holes with $M_{bh} \sim 2 \times 10^6 M_\odot$. In so doing, they cast a solution to two problems: 1) what is the composition of the dark matter; 2) and what is the mechanism which heats the Galactic disk? Their calculation showed that a steady flux of $2 \times 10^6 M_\odot$ black holes passing through the disk would heat the disk in the manner required to explain the velocity dispersion-age relation $\sigma_* \propto t_*^{1/2}$ for disk stars (Wielen 1977).

Although subsequent observational and theoretical work suggests that an explanation of disk heating does not require massive black holes (Carlberg et al 1985; Stromgren 1987; Gomez et al 1990; Lacey 1991)– indeed, analysis of the disk heating problem is ongoing (e.g. Sellwood, Nelson & Tremaine 1998)– one can, in any case, view the disk heating argument as a disk heating *constraint*. The constraint can be developed by generalizing the Lacey & Ostriker model to $M_{bh} > 2 \times 10^6 M_\odot$ with a less-than-unity fraction of halo mass in black holes $f_{bh} < 1$ (e.g. Carr, Bond & Arnett 1984;

Wasserman & Salpeter 1994). Then, since the energy input to the disk $\Delta E \propto M_{bh}^2$ for a single black hole, any combination $f_{bh} M_{bh} \sim 2 \times 10^6 M_\odot$ produces the same net heating of the disk. Therefore $f_{bh} M_{bh} \gtrsim 2 \times 10^6 M_\odot$ overheats the disk and is definitely not allowed. The generalization $f_{bh} < 1$ is desirable, given the variety of dark matter candidates, the results of microlensing surveys (e.g. Alcock et al. 1997) and the fact that not all dark matter need be baryonic given the bound from primordial nucleosynthesis (Pagel 1997).

Are there other constraints on the mass and abundance of black holes in the Galactic halo? In some sense, halo black holes are surprisingly difficult to detect, given that there is considerable observational evidence for black holes of similar mass ($10^6 M_\odot \lesssim M_{bh} \lesssim 10^9 M_\odot$) in the centers of galaxies (e.g. Kormendy & Richstone 1995). Conversely, they have been surprisingly difficult to constrain or rule out. Lacey & Ostriker themselves remarked that the accretion luminosity of such objects may be too high to have escaped detection; however, no definitive constraint has been recorded (Carr, Bond & Arnett 1984; Carr 1994). Hut & Rees (1992) argued that dynamical friction would drag ~ 100 of these objects into the Galactic center in a Hubble time, leading to coalescence and production of a central object much larger than allowed by observational constraints ($M_{bh} \sim 2 \times 10^6 M_\odot$; Genzel et al 1997). However, Xu & Ostriker (1994) tested this argument with detailed N-body simulations and found

that typically only one black hole would remain in the Galactic center due to three-body encounters.

Constraints from gravitational lensing are comparatively weak at this time. For the values of M_{bh} considered in this paper, the large size of the Einstein ring gives event durations orders of magnitude too long for the present Galactic microlensing surveys. Lensing of quasars (Canizares 1982; Kassiola, Kovner, & Blandford 1991) restricts $\Omega_{bh} = \langle \rho_{bh} \rangle / \rho_c$ to be less than about 10%, which is greater than the estimated mass in dark haloes—an upper bound for the scenario we are considering. Several observing plans have been proposed to detect massive black holes. Turner and Umemura (1997) argue that the Sloan Digital Sky Survey and the Hubble Deep Field can place constraints on Ω_{bh} by looking for extremely large amplifications of O and G stars at cosmological distances. Also, Turner, Wardle, & Schneider (1990) propose that $M_{bh} \sim 10^6 M_\odot$ black holes are detectable through arcsecond size lensing of objects in M31 and the Galactic Center.

Wielen (1985,1988) first pointed out that globular clusters also constrain the properties of massive black holes in the Galactic halo because of their susceptibility to external heating and tidal disruption. Later, Moore (1993) applied the same arguments to a set of low mass globular cluster in the halo. These arguments have been re-examined in more detail by Klessen & Burkert (1995) and Arras & Wasserman (1998), who first included cluster evolution due to black hole heating in examining the constraints. Our goal in this and subsequent work will be to re-examine constraints on f_{bh} and M_{bh} imposed by globular clusters using Fokker-Planck calculations of cluster evolution which include the effects of encounters with massive black holes.

Both Wielen (1985,1988) and Arras & Wasserman (1998) delineate two mass regimes for black holes: the low M_{bh} regime, in which individual collisions perturb a cluster only weakly, but where many such collisions produce a steady, diffusive energy input; and the high M_{bh} regime, where a single encounter can destroy the cluster. In the low-mass limit, one can obtain limits on the product $f_{bh} M_{bh}$; in the high-mass limit, one can obtain limits only on f_{bh} for $M_{bh} > M_{high}$. Applying these arguments to Moore’s (1993) cluster sample, Arras & Wasserman (1998) concluded that $f_{bh} M_{bh} \lesssim 10^3 M_\odot$ in the low-mass regime and $f_{bh} \lesssim 0.3$ in the range $10^6 M_\odot \leq M_{bh} \leq 10^7 M_\odot$.

Although Arras & Wasserman (1998) included evolution due to black hole heating, they did not consider the influence of internal relaxation and post-collapse evolution in their calculations. Thus they pointed out the need for improved calculations to derive the most robust constraints on f_{bh} and M_{bh} using the globular cluster argument.

To address this issue in the present work, we combine the statistical framework developed by Arras & Wasserman (1998) with the Fokker-Planck evolutionary calculations employed by Murali & Weinberg (1997a-c). Our calculations include two-body relaxation, post core-collapse evolution and tidal shocking by massive black holes. Using a Monte Carlo approach, we focus on the high-mass regime and directly compute the probabilities for strong collisions between globular clusters and massive black holes.

In order to translate these calculations of the evolution of *individual* clusters into bounds on f_{bh} , we need to consider the implications of our results for the evolution

of a *population* of clusters. To accomplish this, we adopt two different points of view. The first, and more restrictive, viewpoint is that global studies of the evolution of the globular cluster population are consistent with observations assuming *no* black holes at all (e.g. Murali & Weinberg 1997b), so that including black holes should have only a minimal effect. Following this approach, we find that to ensure 50% survival probability for globular clusters with masses $M_c \approx (2.5 - 7.5) \times 10^4 M_\odot$ at $R = 8$ kpc, the fraction of the halo in black holes with masses $M_{bh} \gtrsim (1 - 3) \times 10^6 M_\odot$ must be $f_{bh} \lesssim 0.025 - 0.05$. This limit on f_{bh} is between one and two orders of magnitude stronger than the disk heating constraint at this M_{bh} , and would imply that black holes with $M_{bh} \sim 10^6 M_\odot$ are not a candidate for baryonic dark matter in galactic halos.

Our second approach, which turns out to be systematically less restrictive, examines the evolution and stability of the globular cluster population in the context of a simple model. As we shall see, the two principal effects of perturbations by black holes are to destroy clusters outright, and to cause surviving clusters to lose mass. We model this simply via a partial differential equation that includes mass loss via an advection term, as well as destruction. In order to obtain results valid for black hole masses $\sim 10^6 M_\odot$, we must extend the tidal approximation employed throughout most of this paper, so that non-destructive encounters at impact parameters inside the tidal radius of a cluster may be taken into account. (The extension of our calculations to include such penetrating encounters, as well as more detailed evolutionary models, will be treated by us elsewhere.) In the context of these models, we find that requiring the observed mass distribution of Galactic globular clusters to be stable over ≈ 10 Gyr requires $f_{bh} \lesssim 0.17$ at $R = 8$ kpc for $M_{bh} \gtrsim 2 \times 10^6 M_\odot$. This bound, although not as tight as our more restrictive (and more qualitative) limit on f_{bh} , still implies that massive black holes cannot be the primary constituent of the halo dark matter.

The plan of the paper is as follows. We summarize the framework for determining constraints in §2. In §3 we determine which globular clusters may be considered relatively unevolved over the age of the Galaxy in the absence of bombardment by black holes, and then find the probability that they are destroyed for given values of M_{bh} and f_{bh} . The results are extended to different cluster and black hole parameters using scaling arguments. We then discuss the properties of clusters which are not destroyed outright, but instead undergo many non-destructive collisions over the age of the galaxy. Lastly, in §4 we discuss how our results constrain M_{bh} and f_{bh} .

2 FRAMEWORK

To re-examine constraints on f_{bh} and M_{bh} set by globular clusters, we incorporate collisions and encounters with black holes into multi-mass Fokker-Planck calculations of cluster evolution, which include two-body relaxation and phenomenological binary heating of the core. Our code descends from that of Chernoff & Weinberg (1990). In practice, we take clusters on circular orbits at $R = 16$ kpc: this minimizes the effect of relaxation and allows us to neglect Galactic tidal heating while subjecting clusters to the ap-

proximate black hole-flux crossing the disk. In addition, this radius corresponds to the spatial region containing many of the clusters in the sample used by Moore (1993). See Table 1 below for a list of input parameters for the calculation.

Given that clusters evolve and some will vanish through evolution (e.g. most recently Murali & Weinberg 1997a-c; Gnedin & Ostriker 1997; Vesperini 1997), it is important at the outset to establish which clusters to use in setting constraints. The lifetime for given cluster orbit scales roughly with internal dynamical time t_{dyn} and cluster mass M_c as $t_{life} \propto t_{dyn} M_c$ for quasistatic evolution. Since t_{dyn} scales with Galactocentric position due to tidal limitation, low-mass clusters in the inner Galaxy are the first to vanish. In general, for any particular orbit, there is a minimum mass cluster which survives to the present-day. Clusters with evaporation timescales less than a Hubble time t_H do not provide straightforward constraints on f_{bh} and M_{bh} : clusters currently at or below the minimum mass might have had considerably larger *initial* mass.

It is important to note that the predictions from evolutionary calculations appear quantitatively consistent with observations. The main uncertainty in the Fokker-Planck calculations is the core heating term: calculations predict that clusters have high central densities in the post core-collapse phase, while it is unclear precisely how this relates to observations (e.g. Drukier, Fahlman & Richer 1992). Nevertheless, the predicted death rates are not wildly inconsistent with observations and differences of opinion arise mainly over the importance of evolution in clusters at the peak of the luminosity function, $M_c \sim 10^5 M_\odot$ (Murali & Weinberg 1997b; Gnedin 1997; Harris et al 1998; Kundu et al 1998).

With this in mind, we adopt a two-step approach to investigating constraints on black hole masses: 1) we first determine cluster initial conditions which do not strongly evolve in smooth halos in a Hubble time; 2) we then immerse these clusters in halos with black holes to investigate the possible constraints. While cluster survival is most likely for large M_c , significant perturbation by black holes is most likely for small M_c . We consider cluster masses near the lowest M_c that can survive for 10 Gyr when $f_{bh} = 0$.

2.1 Dynamics of encounters

We specify isotropic distributions of perturbing black holes using the f_{bh} - M_{bh} parameterization: therefore the local number density of black holes $n_{bh}(R) = f_{bh} \rho_{halo}(R) / M_{bh}$. This implies the relative velocity distribution for encounters given in equation (16) of Arras & Wasserman (1998).

Encounters between clusters and black holes are predominantly impulsive given the Galactic rotation velocity $V_c \sim 220 \text{ km s}^{-1}$. For a cluster at $R \sim 16 \text{ kpc}$, the characteristic internal velocity $v_{int} \sim 5 \text{ km s}^{-1}$. For a cluster on a circular orbit at V_c and a random perturber drawn from a non-rotating, isothermal halo, the typical relative encounter velocity $V_{rel} \sim V_c$. For the black hole masses and abundances considered below, the influence of impacts at ~ 10 tidal radii, r_t , is small. Even at this distance, the timescales $r_t / v_{int} \gg 10 r_t / V_c$ so the probability of a non-impulsive encounter is very small.

To perform the simulations described below, we incorporate individual collisions between black holes and globular

clusters into Fokker-Planck calculations using the impulse approximation. To determine the effect of each encounter, we calculate the second-order change in the distribution function (e.g. Murali & Weinberg 1997a). The method is similar to procedures used by Murali & Weinberg (1997a) and Gnedin & Ostriker (1997) in studies of cluster evolution in the Galactic tidal field. However, in the appendix, we show that there is a small error in the previous treatments. Our current treatment remedies this.

This approach represents a linearization of the full collision problem. In complete generality, the collision problem requires simultaneous solution of the coupled, collisionless Boltzmann-Poisson equations. Linearization imposes a limited range of validity. In the appendix, we show that this approach is valid for $dM/M \lesssim 0.15$ in a single encounter. We terminate any calculation where $dM/M \geq 0.15$.

We adopt the Fokker-Planck approach, rather than, say, N-body simulations because we can study evolution due to both internal and external effects and because we need a computationally feasible method to conduct the Monte Carlo simulations described below. While N-body simulations permit fully non-linear calculations of strong collisions, it is difficult to include two-body relaxation, core heating which leads to post core-collapse evolution and the effect of weak encounters in which only small mass loss occurs. N-body simulations are also much too expensive to use in Monte Carlo simulations.

2.2 High-mass limit

Our analysis focuses on the *high-mass limit* for halo black holes (e.g. Bahcall, Hut & Tremaine 1980; Wielen 1985; Arras & Wasserman 1998). The limiting mass is defined as the mass for which a single, tidal encounter at the typical relative velocity can destroy a cluster. For completeness, we sketch the definition of the high-mass limit following the detailed discussion given by Arras & Wasserman (1998).

Let us assume that cluster destruction occurs when a strong collision unbinds a fraction dM of the total mass. As shown in Appendix A, the fractional mass loss in the impulsive tidal limit

$$|dM/M| \equiv f = K M_{bh}^2 / V_{rel}^2 b^4 \quad (1)$$

where b and V_{rel} are the impact parameter and relative velocity of the collision. The constant

$$K = \frac{\kappa G^2 \langle r^2 \rangle}{\sigma^2} \quad (2)$$

The quantity $\langle r^2 \rangle$ is the mean square radius of the cluster, σ is its one-dimensional central velocity dispersion and κ is a dimensionless constant depending only on its structure; see Arras & Wasserman 1998, equations (36) and (37). Note that, from the virial theorem, $\sigma^2 \propto r_t^{-1}$ and that, by tidal limitation in an isothermal sphere, $r_t \propto R^{2/3}$, so that $K \propto R^2$, where R is the Galactocentric radius.

Rewriting this, we may define the ‘destructive radius’:

$$b_d = \left(\frac{K M_{bh}^2}{V_{rel}^2 f_d} \right)^{1/4}, \quad (3)$$

where f_d is the fractional mass loss leading to destruction. Given a black hole of mass M_{bh} moving at velocity V_{rel}

with respect to the cluster, an encounter with any impact parameter $b \leq b_d$ leads to fractional mass loss $f \geq f_d$ from the cluster. Of course, since the black hole can travel with a range of relative velocities in relation to the cluster, we may invert this relation to define the range in V_{rel} which leads to destructive encounters within r_t :

$$V_{rel} \leq \left(\frac{KM_{bh}^2}{f_d r_t^4} \right)^{1/2} \equiv V_{rel,max} \quad (4)$$

In general, cluster properties depend on time, so that b_d and $V_{rel,max}$ will too.

We define the limiting mass $M_{bh} \equiv M_{high}$ to be the black hole mass for which $f_d = 0.15$ in an encounter at $b = r_t$ with $V_{rel} = 2.5 \langle V_{rel} \rangle$, where $\langle V_{rel} \rangle \approx 1.47V_c$. The factor of 2.5 is introduced to ensure that the probability of non-destructive collisions inside r_t is very small. (The factor of 2.5 is probably larger than it needs to be: we estimate a probability of about 10^{-5} for a nondestructive collision inside r_t when $M_{bh} = M_{high}$ with this choice.) Note that $(b_d/r_t)^2 = M_{bh}/M_{high}$ for this value of V_{rel} , and, more generally, $(b_d/r_t)^2 = 2.5 \langle V_{rel} \rangle M_{bh}/V_{rel} M_{high}$.

2.3 Monte Carlo enumeration of collision probabilities

To proceed, we introduce a framework for calculating the probability that a cluster experiences an encounter with fractional mass loss f_d in a Hubble time. For the black hole background specified above, the rate of encounters with $f \geq f_d$ is

$$\frac{\partial N_d}{\partial t} = 2\pi \int_0^\infty dV_{rel} \int_0^{b_d} dbb V_{rel} n_{bh}(R) F(V_{rel}, t) \equiv \Gamma_d, \quad (5)$$

where $F(V_{rel}, t)$ is the relative velocity distribution of the black hole population with respect to the instantaneous motion of the cluster. For a non-evolving cluster on a circular orbit, Arras & Wasserman (1998) show that

$$N_d = \pi T \rho_{bh}(R) \left(\frac{K}{f_d} \right)^{1/2}. \quad (6)$$

Implicit in equation (6) are a number of noteworthy scalings: N_d is actually independent of $M_{bh} \geq M_{high}$ and M_c , and $N_d \propto R^{-1}$ given f_{bh} . In general, the probability that a cluster suffers an encounter with $f \geq f_d$ in a Hubble time is

$$P_d = 1 - \exp(-N_d). \quad (7)$$

Qualitatively, $N_d \lesssim 1$ is required for a cluster to avoid a single, destructive encounter with a black hole.

In the present work, our goal is to determine P_d using realistic calculations of cluster evolution: namely the Fokker-Planck solutions discussed above. As mentioned above, the method is linear and valid only for $f \leq 0.15$. Therefore, if we take $f_d = 0.15$, then it is most appropriate to call P_d the *probability for a strong collision*. However, we also refer to P_d as the disruption probability according to its original definition.

Since we are concerned with the probability that a cluster does or does not suffer *one* such collision, the range of possible final cluster states is broad: in other words, the evolution is stochastic. We therefore calculate collision probabilities using Monte Carlo simulations.

Each simulation has 60 realizations. The collision history for each realization is obtained by direct sampling of the relative velocity distribution and space density of black holes of mass M_{bh} within 10 initial tidal radii of the cluster. The disruption probability is calculated directly from the fraction of the 60 runs in which an encounter with $f \geq 0.15$ occurs. Initially, each cluster has mass M_c , King parameter W_0 , galactocentric radius R and additional parameters (internal mass spectrum: Murali & Weinberg 1997b,c) given in Table 1.

3 CONSTRAINTS FROM GLOBULAR CLUSTERS

3.1 Cluster evolution in a smooth halo: $f_{bh} = 0$

For $f_{bh} = 0$, our calculations include only relaxation and post-collapse heating of the core. Table 2 gives the evaporation times t_{evap} for clusters on circular orbits at $R_{gc} = 16$ kpc. The evaporation time is roughly 10 Gyr $\equiv t_H$ for $M_c \sim 10^4 M_\odot$, independent of concentration and roughly proportional to the initial mass of the cluster. The evaporation times scale as $t_{evap}(R) = t_{evap}(R/16 \text{ kpc})$ for an isothermal halo. The lack of dependence on concentration is also seen in calculations presented by Lee et al (1991) and Gnedin & Ostriker (1997).

From these results, we conclude that clusters with initial masses $M_c = 2.5 \times 10^4 M_\odot$ and $7.5 \times 10^4 M_\odot$ provide appropriate specimens to study under bombardment by black holes: at this radius, they have $t_{evap} \gg t_H$ for $f_{bh} = 0$; the low-mass cluster lets us probe the lowest values of M_{high} while the high-mass cluster is farther from the evaporation boundary, thus giving greater confidence in the conclusions.

3.2 Collision probabilities in lumpy halos: $f_{bh} > 0$

Our main calculations depict the evolution of King model clusters on circular orbits at $R_{gc} = 16$ kpc with a range of concentration and mass. We take halos with a range of f_{bh} and $M_{bh} = M_{high}$, where M_{high} depends on the initial concentration and mass of the cluster. Figures 1-3 compare the results of the Monte Carlo calculations with the analytic predictions for the fixed cluster potential (equation 7). There appear to be statistical fluctuations in the Monte Carlo results as well as a small systematic trend for 15% collision probabilities to lie below the fixed cluster predictions. Error bars are 68% confidence regions found using Bayesian methods (as in Arras & Wasserman 1998) and are only statistical. Overall, however, the agreement is surprisingly good given that the analytic prediction neglects changes in the cluster potential due to internal evolution.

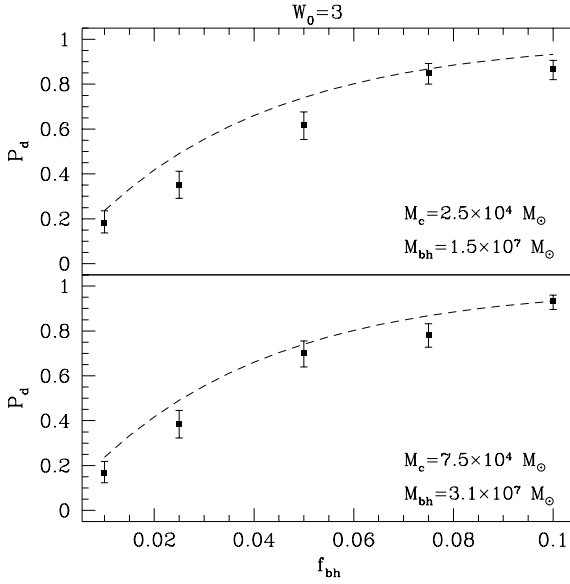
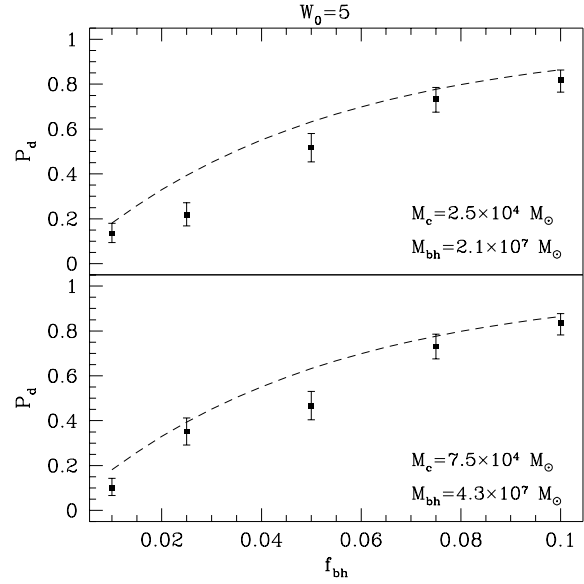
Lower P_d might be expected in the simulations because two-body relaxation hardens the potential while mass loss reduces the cross-section for collisions. Although evolution should help clusters avoid strong collisions, P_d is only reduced by roughly 10-20% for $f_{bh} \lesssim 0.1$. Agreement is best at the smallest and largest f_{bh} . Agreement at $f_{bh} \rightarrow 0$ is trivial, as $P_d \rightarrow 0$ in that limit. The agreement at larger f_{bh} , where $P_d \rightarrow 1$, arises because the expected time to the first destructive encounter is small, so evolution (and the resulting increase in concentration) is relatively unimportant.

Table 1. Cluster Initial Conditions

Structure		Adopted values
M_c	total mass	$2.5 \times 10^4, 7.5 \times 10^4 M_\odot$
W_0	King concentration parameter	$W_0 = 3, 5, 7$
R_c	cluster limiting radius	set to tidal limit r_t
t_{rh}	initial half-mass relaxation time	$2 - 6 \times 10^9$ yr
Internal mass spectrum		
β	mass spectral index: $N(m) \propto m^{-\beta}$	$\beta = 2.35$ (Salpeter)
m_l	lower mass limit	$m_l = 0.1 M_\odot$
m_u	upper mass limit	$m_u = 2.0 M_\odot$
Orbit:		circular at 16 kpc

Table 2. Evaporation times at 16 kpc (in Gyr)

$M_c(M_\odot)/W_0$	3	5	7
1×10^3	1.2	1.2	1.2
2.5	2.6	2.7	2.7
5.0	4.6	4.7	4.7
7.5	6.6	6.7	6.8
1×10^4	8.5	8.5	8.8
2.5	20	21	21
5.0	38	40	40
7.5	55	59	59
1×10^5	73	78	77


Figure 1. Probabilities for 15% encounters for $W_0 = 3$ clusters with indicated masses at 16 kpc where $M_{bh} = M_{high}$. Solid squares with associated error bars show the results of Monte Carlo simulations; dashed line shows the analytic prediction determined from equations (6) and (7).

Figure 2. Probabilities for 15% encounters for $W_0 = 5$ clusters with indicated masses at 16 kpc where $M_{bh} = M_{high}$. Solid squares with associated error bars show the results of Monte Carlo simulations; dashed line shows the analytic prediction determined from equations (6) and (7).

Nevertheless, the agreement between the analytic formulae and simulations is surprisingly good even for intermediate values, $f_{bh} \sim 0.05$, where $P_d \sim 0.3 - 0.5$.

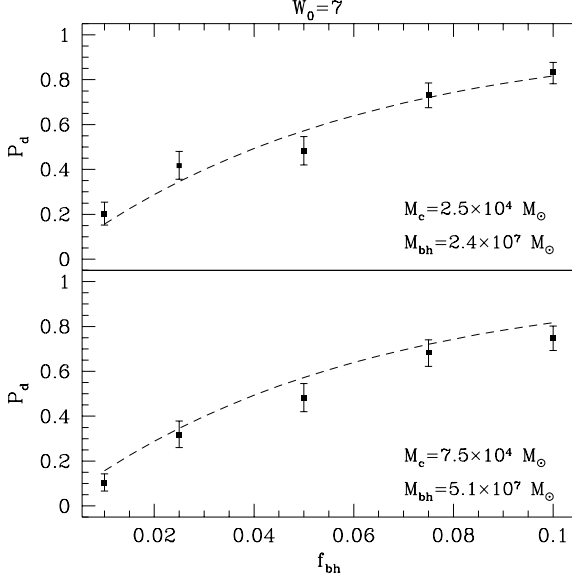


Figure 3. Probabilities for 15% encounters for $W_0 = 7$ clusters with indicated masses at 16 kpc where $M_{bh} = M_{high}$. Solid squares with associated error bars show the results of Monte Carlo simulations; dashed line shows the analytic prediction determined from equations (6) and (7).

3.2.1 Independence of $M_{bh} > M_{high}$

To see how cluster evolution affects P_d at higher M_{bh} , we repeat the above calculations for $W_0 = 5$ and $M_{bh} = 2M_{high}$. Figure 4 shows the results. They agree well with the results for $W_0 = 5$ presented in the previous section. We conclude that evolutionary effects do not destroy the high-mass scaling derived in the fixed cluster approximation. This, in fact, is not surprising since we have restricted our attention to clusters with $t_{ev} > t_H$.

3.2.2 Approximate behavior for $M_{bh} < M_{high}$

In the above analysis, we have conservatively adopted a very large choice for M_{high} to ensure that our calculations obey the high-mass formalism in the strictest sense. However, Arras and Wasserman (1998) have shown that the tidal limit formula for mass loss provides a good approximation even when $b_d < r_t$ since clusters have fairly extended, loosely bound halos. Typically we expect the tidal formula to remain fairly accurate even for impacts just outside the core radius ($b_d/r_t \sim 0.1$ for $W_0 = 5$). This approximation is worst at low concentration because the mass distribution is more extended. The approximation improves as the cluster evolves and becomes more concentrated. For example, $b_d = 0.25r_t$ encloses roughly 50% of the mass in the $W_0 = 3$ cluster and roughly 80% of the mass in the $W_0 = 7$ cluster.

For fixed N_d and $V_{rel,max} = 2.5\langle V_{rel} \rangle$, $M_{bh} \propto b_d^2$. Thus the approximation significantly improves the limiting M_{bh} which our calculations explore. In particular, if we adopt $b_d = 0.25r_t$, then our calculations are valid for $M_{bh} = 0.0625M_{high}$. In other words the high-mass scaling obtains for $M_{bh} \ll M_{high}$ which we have defined above.

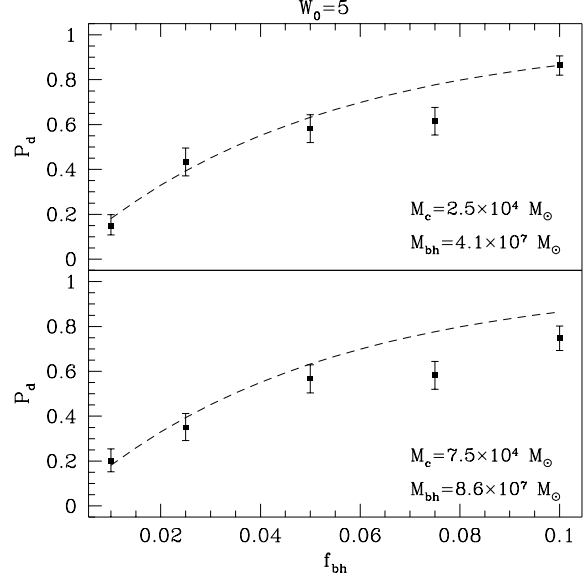


Figure 4. Probabilities for 15% encounters for $W_0 = 5$ clusters with indicated masses at 16 kpc where $M_{bh} = 2M_{high}$ for M_{high} used in figures 1-3. Solid squares with associated error bars show the results of Monte Carlo simulations; dashed line shows the analytic prediction determined from equations (6) and (7).

Figure 5 shows the collision probabilities calculated using this approximation. The results agree well with the analytic predictions and indicate that the high-mass or destructive regime obtains down to $M_{bh} \sim 10^6 M_\odot$.

3.2.3 Radial scaling of collision probabilities

The collision probabilities enumerated for $R = 16$ kpc can be scaled approximately to larger radius by keeping N_d fixed. Since $\rho_{halo} \propto R^{-2}$ and $K \propto R^2$ from equation (2), then N_d is constant with radius for $f_{bh} \propto R$. The scaling is approximate because the intrinsic evolutionary rate of a cluster varies with radius due to the variation in dynamical time: $t_{dyn} \propto R$ for a tidally limited cluster in an isothermal halo. However, the above calculations fall into the regime $t_{evap} > t_H > \Gamma_d^{-1}$, so the scaling is strong. Additional calculations verify the scaling.

3.2.4 Eccentricity dependence

Clusters on eccentric orbits in the Galaxy experience time variation in Γ_d , the rate of destructive encounters, since the number density of black holes varies along their orbits. The galactic tidal force also varies along a cluster orbit; this can be accounted for roughly by assuming that the cluster is tidally limited at the pericenter of its orbit. The integrated number of destructive encounters can then be written $N_d = N_d(\epsilon = 0)\mathcal{C}(\epsilon)$, where $\epsilon = 1 - J/J_{max}(E)$ is a measure of the eccentricity of an orbit with energy E and angular momentum J , and $N_d(\epsilon = 0)$ is the number of destructive encounters for a circular orbit with energy E (and angular momentum $J_{max}(E)$).

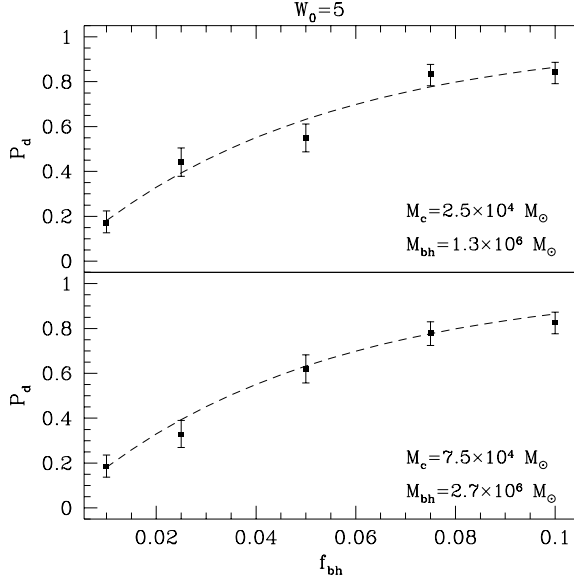


Figure 5. Probabilities for 15% encounters for $W_0 = 5$ clusters with indicated masses at 16 kpc where $M_{bh} = 0.0625M_{high}$ for M_{high} used in figures 1-3. Solid squares with associated error bars show the results of Monte Carlo simulations; dashed line shows the analytic prediction determined from equations (6) and (7).

Whether or not N_d increases or decreases with increasing eccentricity depends on a competition between a higher number of encounters at smaller R , and more time spent at large R near apocenter. By numerical evaluation of \mathcal{C} , we have found that $\mathcal{C} \lesssim 1$, so that the penalty of spending more time at apocenter with the accompanied small encounter rate is the dominant factor. A convenient analytical formula for $\mathcal{C}(\epsilon)$ can be found by expanding the integral $N_d(t) = \int_0^t dt' \Gamma_d(t')$ for small ϵ and integrating t' over an integral number of orbital periods – a good approximation if many orbits have been traversed. Under these conditions we find

$$\mathcal{C}(\epsilon) \simeq 1 - \frac{3}{2}\epsilon^{1/2} + \frac{33}{24}\epsilon + \mathcal{O}(\epsilon^{3/2}). \quad (8)$$

The probability of survival is larger for clusters on eccentric orbits than for clusters on circular orbits, given E . For example, consider two clusters with the same orbital energy, one on a circular orbit at $R = 16$ kpc and a second on an eccentric orbit with pericenter at $R_p = 8$ kpc; in this case N_d is smaller for the eccentric orbit by about a factor of two. In this case, the cluster on the eccentric orbit has a higher rate of internal evolution because of its smaller pericenter, an effect which must also be taken into account; we discuss qualitatively in §4. Finally, we note that the average value of the correction factor for an isotropic distribution of angular momenta is $\langle \mathcal{C}(\epsilon) \rangle \simeq 0.5$ for a fairly large range of orbital energies.

3.3 Properties of evolved clusters

We examine the basic properties of the clusters which do not undergo 15% collisions. Thus we describe the effect of the

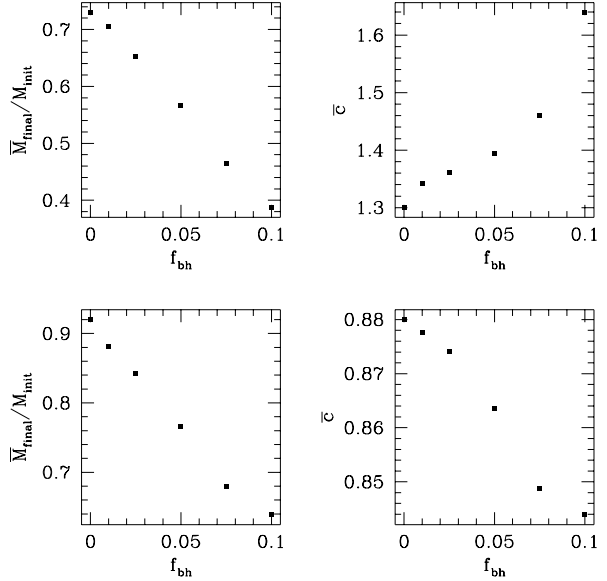


Figure 6. Mean final mass and concentrations of $W_0 = 3$ clusters which *do not* suffer 15% collisions. Top row shows results for clusters with $M_{init} = 2.5 \times 10^4 M_\odot$; bottom row shows results for clusters with $M_{init} = 7.5 \times 10^4 M_\odot$.

weaker encounters on cluster evolution. Ideally we would like to determine the Green’s function or probability amplitude for evolution from a given initial state to a given final state (e.g. Arras & Wasserman 1998). Of course, with 60 realizations per run and only the fraction $1 - P_d(f_{bh})$ not suffering strong collisions, we can only understand the distribution of final states very approximately. To do so, we simply examine the mean mass and concentration of the ‘surviving’ clusters.

Figures 6-8 show the mean mass and concentration for clusters in the runs discussed above. In each case, remaining mass decreases monotonically with f_{bh} . As mentioned above, the black hole flux leads to both weak and strong encounters: clusters which do not suffer strong collisions still lose mass through weak encounters, so the final mass will be less than that of an isolated cluster.

The evolution of concentration $c = \log r_t/r_c$ behaves somewhat differently in each case. At low mass, the relaxation rate is enhanced by weak encounters for all initial concentrations. However, the $W_0 = 3$ clusters have not yet entered core collapse so c increases monotonically with f_{bh} . For $W_0 = 5$ and $W_0 = 7$, c decreases with f_{bh} because the core reaches the post-collapse stage of expansion more rapidly due to the external heating.

At high mass, the effect differs because of the longer intrinsic relaxation time. For initial $W_0 = 3$, c decreases with f_{bh} because heating has little effect on core evolution, tending only to decrease r_t . For $W_0 = 5$, c increases with f_{bh} due to the acceleration of core evolution by external heating. For $W_0 = 7$, external heating accelerates core evolution past collapse and into expansion, so that c decreases with f_{bh} .

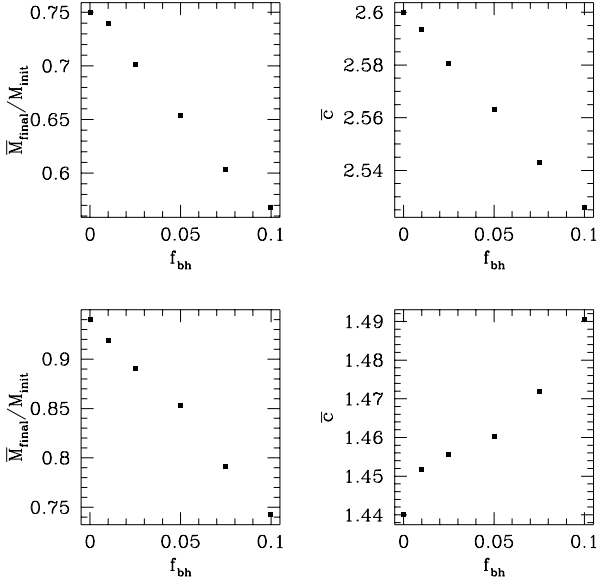


Figure 7. Mean final mass and concentrations of $W_0 = 5$ clusters which *do not* suffer 15% collisions. Top row shows results for clusters with $M_{init} = 2.5 \times 10^4 M_\odot$; bottom row shows results for clusters with $M_{init} = 7.5 \times 10^4 M_\odot$.

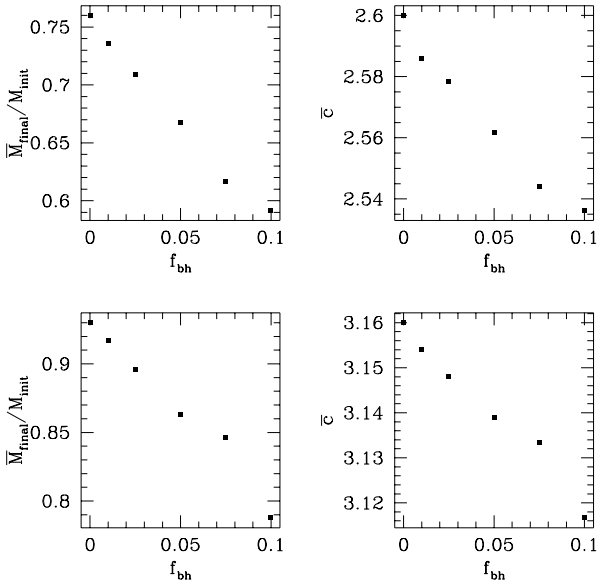


Figure 8. Mean final mass and concentrations of $W_0 = 7$ clusters which *do not* suffer 15% collisions. Top row shows results for clusters with $M_{init} = 2.5 \times 10^4 M_\odot$; bottom row shows results for clusters with $M_{init} = 7.5 \times 10^4 M_\odot$.

4 DISCUSSION

We have examined in detail how typical globular clusters evolve in a halo which contains a population of massive black holes with $M_{bh} \sim 10^6 M_\odot$. Our main goal was to establish probabilities for strong collisions between clusters and black holes in the high-mass limit using Fokker-Planck cal-

culations in order to combine effects of internal relaxation, binary heating and black hole shocking.

Our results show that evolution does not radically alter collision probabilities determined in the fixed cluster approximation (equation 7). This result is not surprising given our approach: we first determine initial conditions which do not lead to significant evolution in the absence of black holes; we then include black holes of some mass M_{bh} and abundance f_{bh} in calculations with these initial conditions. Evolution can help reduce P_d , but weaker encounters tend to accelerate core collapse and evaporation by removing mass from the halo. The differences that do arise are relatively small and therefore will not affect any conclusions we draw below.

In calculating P_d , we have only considered clusters on circular orbits. As discussed in §3.2.4, clusters on eccentric orbits have lower collision probabilities. However, decreasing the pericenter also shortens the evaporation time for a cluster in isolation. For example, Table 2 shows that a cluster with mass $M_c = 2.5 \times 10^4 M_\odot$ has an evaporation timescale of about 20 Gyr assuming a circular orbit of radius $R = 16$ kpc; if its pericenter were $R_p = 8$ kpc, its evaporation time would be about 10 Gyr. Moreover, disk shocking becomes effective for pericenter radii $R_p \lesssim 8$ kpc, further reducing the odds of survival for $M_c = 2.5 \times 10^4 M_\odot$ even if $f_{bh} = 0$. To be conservative, we could avoid these complications by focusing on clusters of larger mass, resulting in correspondingly larger values of the minimum black hole mass on which we can place constraints in the high-mass limit: for a fixed evaporation time, and assuming tidally limited clusters, we should scale $M_c \propto R_p^{-1}$ and $M_{high} \propto M_c^{2/3} R_p^{1/3} \propto R_p^{-1/3}$, approximately. If we choose to be bolder, we could keep M_c fixed, restrict ourselves to acceptable values of R_p (e.g. $R_p \gtrsim 8$ kpc for $M_c = 2.5 \times 10^4 M_\odot$) and rescale $M_{high} \propto R_p^{1/3}$. Either way, the limits on f_{bh} are unlikely to change by more than a factor of two (see §3.2.4). Because we have only rigorously considered clusters on circular orbits, we will address any remaining ambiguities in defining M_{high} in our next paper (Arras et al 1999), where we shall consider the evolution of a realistic population of globular clusters and work our way up from the regime of low black hole masses, thereby obtaining limiting values of f_{bh} as a function of M_{bh} ; where that curve asymptotes to the M_{bh} -independent bound found here will determine M_{high} .

We have calculated P_d assuming $f_d = 0.15$; this restriction was imposed by the limitations of our linear perturbation procedure. We can scale the results to higher f_d to consider collisions more likely to disrupt the cluster, i.e., $f_d \sim 0.5$. Here nonlinear effects become important but the scaling approximately holds. In linear theory, $N_d \propto f_{bh}/\sqrt{f_d}$ from equation (6) while $M_{high} \propto \sqrt{f_d}$. Therefore, for fixed f_{bh} , $N_d \propto 1/\sqrt{f_d}$ and the values of P_d calculated above decrease correspondingly for $f_d > 0.15$. For fixed N_d and P_d , $f_{bh} \propto \sqrt{f_d}$. (Note that if $N(f'_d) \sim 1$, then for $f_d < f'_d$, $N_d(f_d) \sim \sqrt{f'_d/f_d}$, which would only result in a fractional mass loss $\sim \sqrt{f'_d f_d} < f'_d$; large fractional mass loss in a single encounter is always more likely than in numerous encounters each with smaller fractional mass loss.)

We can also scale to different galactocentric radii using the approximate relationships $f_{bh} \propto R$ (see §3.2.3) and $M_{high} \propto f_d^{1/2} M_c^{2/3} R^{1/3}$, which becomes $M_{high} \propto f_d^{1/2} R^{-1/3}$ for fixed evaporation time (see §3.2.4); including disk shock-

ing – which we have neglected here – ought to raise the value of M_{high} somewhat because only higher mass clusters survive. The constraints on f_{bh} become stronger for smaller galactocentric radii, but we expect f_{bh} to be nonuniform as a consequence of dynamical friction, so limits at relatively large R are easiest to interpret.

4.1 Interpreting the collision probabilities

Our calculations in smooth halos, $f_{bh} = 0$, combined with the observational picture serve as a guide for interpreting the collision probabilities. Observationally, the similarity of globular cluster luminosity functions over a range of galaxy environments (e.g. Harris 1991) may reflect the formation process and suggests that cluster populations are relatively unevolved for $M_c \sim 10^5 M_\odot$. Moreover, the flatness of the distribution of globular cluster luminosities, dN/dL_c – and hence dN/dM_c – at low L_c in the Milky Way (e.g. Ashman & Zepf 1998) suggests that globular clusters with $M \lesssim 10^5 M_\odot$ are not whittled away rapidly, but are relatively long-lived since, otherwise, the rate of destruction would far exceed the rate of production and the distribution would fall off drastically. Our calculations with $f_{bh} = 0$ appear to be reasonably consistent with this expectation. In particular, these calculations show that clusters on circular orbits at 16 kpc survive beyond a Hubble time for $M \gtrsim 10^4 M_\odot$, incurring roughly 25% mass loss for $M_c = 2.5 \times 10^4 M_\odot$ and roughly 5% mass loss for $M_c = 7.5 \times 10^4 M_\odot$. A stringent view, therefore, requires that halo black holes leave these clusters relatively unscathed.

Our numerical simulations show that the probability of a collision with $f_d = 0.15$ is about 30-40% for $f_{bh} \approx 0.025$, about 50% for $f_{bh} \approx 0.05$, and about 80% for $f_{bh} \approx 0.1$; assuming that the collision probability in this range of f_{bh} is excessive, we can rule out $M_{bh} \gtrsim 1.3 \times 10^6 M_\odot$ for $M_c = 2.5 \times 10^4 M_\odot$ and $M_{bh} \gtrsim 2.7 \times 10^6 M_\odot$ for $M_c = 7.5 \times 10^4 M_\odot$ for $f_{bh} \gtrsim 0.1$. From the scaling $N_d \propto f_{bh}/\sqrt{f_d}$, equal collision probabilities for $f_d = 0.5$ imply the values $f_{bh} = 0.05$, $f_{bh} = 0.09$ and $f_{bh} = 0.18$, respectively; since $M_{\text{high}} \propto \sqrt{f_d}$ (see Section 2.2, especially eq. [3]), these limits apply to $M_{bh} \gtrsim 2.4 \times 10^6 M_\odot$ for $M_c = 2.5 \times 10^4 M_\odot$ and $M_{bh} \gtrsim 4.9 \times 10^6 M_\odot$ for $M_c = 7.5 \times 10^4 M_\odot$. These are somewhat higher but still very restrictive.

Black hole collisions do not only destroy clusters, but also whittle away their masses. For low $f_d N_d$, the fractional mass loss endured by surviving clusters is approximately $f_d N_d$ in the tidal limit (Figs. 6-8 and Arras & Wasserman 1999). Thus, we expect that for large $f_d N_d$, the mean mass per cluster declines like $\exp(-f_d N_d)$, and the total mass in clusters declines like $\exp[-(1+f_d)N_d]$ when cluster destruction is taken into account, in the tidal limit. To a first approximation, the evolution of the distribution of clusters must account for a steady advection downward in mass as well as destruction. If $N(M, t)dM$ is the number of clusters with masses between M and $M + dM$ at time t , then

$$\frac{\partial N(M, t)}{\partial t} = -\Gamma_d N(M, t) + \Gamma_d f_d \frac{\partial [N(M, t)M]}{\partial M} \quad (9)$$

represents a simple advection-destruction model appropriate for the tidal limit. The solution to this equation is

$$N(M, t) = \exp[-\Gamma_d(1-f_d)t]N(M \exp(f_d \Gamma_d t), 0). \quad (10)$$

According to this solution, the total number of clusters declines $\propto \exp(-\Gamma_d t) = \exp(-N_d)$ and the total mass remaining in clusters after time t is $\propto \exp[-\Gamma_d(1+f_d)t] = \exp[-(1+f_d)N_d]$.

For a given black hole mass M_{bh} , the tidal approximation holds up to some maximum cluster mass, M_t ; if attention is restricted to the tidal approximation, which considers only collisions with impact parameters outside r_t , this maximum mass is $M_t \sim (\text{a few}) \times 10^4 M_\odot$ for $M_{bh} = 10^6 M_\odot$.

Black hole collisions still destroy and whittle away clusters with masses above M_t . Consequently, clusters destroyed and chiselled away at masses below M_t are replaced, to a degree, by clusters originally at masses above M_t . Our calculations in the tidal limit cannot describe this evolutionary process; to do so requires calculations of what happens as a consequence of black hole collisions at $b < r_t$, which we have excluded in this paper (but are in the midst of calculating, and will publish separately). However, from earlier work (e.g. Arras & Wasserman 1999), we already know that the tidal approximation continues to describe the mean mass loss by a cluster to within 20-30% for somewhat smaller impact parameters, $b \gtrsim (0.1 - 0.2)r_t$. A quantitatively reasonable interpolation formula for the fractional mass loss of a cluster due to a collision with a black hole passing within impact parameter b of the center of a cluster at relative speed v_{rel} is

$$f(b, v_{rel}) = \frac{f(0, V_c)(V_c/v_{rel})^2}{[1 + (b/b_0)^2]^2}, \quad (11)$$

where $f(0, V_c)$ is the fractional mass loss at zero impact parameter for relative velocity $v_{rel} = V_c$; for a tidally limited cluster at galactocentric radius r , $f(0, V_c) \propto M_{bh}^2/M^{4/3}r^{2/3}$. The numerical value of $f(0, V_c)$ can be found using the results of Arras & Wasserman 1999 (see fig.3). The value of b_0 is fixed by requiring the rate of destructive encounters found using eq.11 give the correct tidal limit.

For a given black hole mass, there is a new critical mass M_d above which clusters become considerably more immune to destruction. Typical penetrating encounters are nondestructive when the cluster mass is large enough that $f(0, V_c) < f_d$. Using eq. (11), we estimate

$$M_d \approx 2 \times 10^5 M_\odot \left(\frac{M_{bh}}{10^6 M_\odot} \right)^{3/2} \left(\frac{8 \text{ kpc}}{R} \right)^{1/2} \left(\frac{0.5}{f_d} \right)^{3/4}. \quad (12)$$

The evolution of clusters with $M > M_d$ in the face of black hole collisions is described poorly by the tidal approximation for two reasons. First, the rate of destructive encounters is low, because $f(0, V_c)$ drops below f_d for $M > M_d$. Second, the rate at which cluster advect downward in mass is slowed because of the same cutoff in fractional mass loss. We can generalize eq. (9) to account for the different behavior at masses above and below M_d ; the resulting equation is

$$\begin{aligned} \frac{\partial N(M, t)}{\partial t} &= -\Gamma_d I(M/M_d)N(M, t) \\ &+ \Gamma_d f_d \frac{\partial [N(M, t)MH(M/M_d)]}{\partial M}, \end{aligned} \quad (13)$$

where, from the scalings implied by eq. (11), we infer that $I(z) \rightarrow 1$ for $z \ll 1$ and $I(z) \rightarrow 0$ for $z \gg 1$, and $H(z) \rightarrow 1$ for $z \ll 1$ and $H(z) \sim z^{-2/3}$ for $z \gg 1$. (The exact M/M_d dependences can be computed from eq. [11] given the distribution of V .)

The tidal limit is recovered for essentially the entire range of globular cluster masses for sufficiently large M_{bh} . The most massive Galactic globular cluster, ω Cen, has $M_c \approx 2.4 \times 10^6 M_\odot$ (e.g. Ashman & Zepf 1998, Mandushev et al. 1991), and $M_d > 2.4 \times 10^6 M_\odot$ for $M_{bh} > 5.2 \times 10^6 M_\odot (R/8 \text{ kpc})^{1/3} (0.5/f_d)^{1/2}$ from eq. (12). Since cluster masses decrease with time as a result of black hole perturbations, M_{bh} must be somewhat larger still for the tidal approximation to hold for all time.

According to the advection-destruction solution, eq. (10), the cluster mass distribution evolves self-similarly with time in the tidal limit, which means that the initial conditions must have resembled the distribution seen today, except shifted to larger mass. Thus, we cannot use the shape of the distribution to derive a bound on f_{bh} , without additional information on the initial mass function for clusters, and without including other processes, such as evaporation and (at $R \lesssim 8$ kpc) disk shocking. * Requiring that the total mass lost by clusters not exceed about 100 times the total mass presently contained in them, so the halo star population is not primarily due to ejecta from clusters (e.g. Klessen & Burkert 1996 and references therein), implies $N_d \lesssim 3.1$, or $f_{bh} \lesssim 0.36(R/16 \text{ kpc})$, for $f_d = 0.5$. This limit is fairly conservative, since metallicity differences suggest that the bulk of halo field stars did not originate from globular clusters (Harris 1991). Moreover, clusters on nearly circular orbits are somewhat likelier to be disrupted than clusters on elongated orbits, so we should expect ejected stars to have a tangentially-biased velocity ellipsoid in the inner Galaxy, which is not observed for the halo stars (Beers & Sommer-Larson 1995).

For smaller M_{bh} , for which M_d falls in the range of present (and past) cluster masses, we can use eq. (13) to get a rough idea of how the cluster distribution function evolves as a consequence of bombardment by massive black holes. (We shall present more realistic and accurate models, as well as statistical analyses, in a subsequent paper.) Qualitatively, clusters with masses below M_d ought to lose mass and be destroyed rapidly. Clusters with masses above M_d are less prone to destruction, and lose mass more slowly. Although the advection of clusters from masses above M_d to below M_d ought to replenish the supply of low mass clusters lost to destructive collisions, the slowness of the process results in an overall truncation of $N(M, t)$ at low values of M .

To explore the stability of the presently-observed mass distribution of clusters, we used eq. (13) to compute the evolution of a distribution that is originally

$$N(M, 0) = \frac{1}{M_0(1 + M/M_0)^2}, \quad (14)$$

with $M_0 = 3 \times 10^5 M_\odot$, up to a maximum mass $M_{max} = 10^7 M_\odot$; the calculations assumed $f_d = 0.5$ and $M_d = 6 \times 10^5 M_\odot$ (corresponding to $M_{bh} = 2 \times 10^6 M_\odot$). The original cluster mass distribution given by eq. (14) is flat below

* Since the evaporation time scales $\propto M$, the rate of evaporative mass loss, \dot{M}_{ev} , is approximately independent of mass, and the tidal limit solution with evaporation is $N(M, t) = \exp[-(1 - f_d)t]N(M_i(t), 0)$, with $M_i(t) = M \exp(f_d \Gamma_d t) + (M_{ev}/\Gamma_d f_d)[\exp(f_d \Gamma_d t) - 1]$. Evaporation can be included similarly in solving eq. (13). In deriving limits on f_{bh} , we neglect evaporation, which would make our constraints slightly tighter.

M_0 and $\propto M^{-2}$ above, in reasonable agreement with the observed luminosity function for globular clusters in the Milky Way (and other galaxies), assuming a constant $M/L \approx 3$ (e.g. Ashman & Zepf 1998). The results for $MN(M, t)$, the distribution of clusters in $\ln M$, is shown in Fig. 9a; the logarithmic slope $\partial \ln N(M, t)/\partial \ln M$ is shown in Fig. 9b. These figures illustrate the truncation of the distribution at low masses, and show how the shape of the distribution tends to evolve with time. From Fig. 9b, we see that the shape begins to deviate significantly from the original one after $\Gamma_d t = N_d \approx 2$ or 3. Although this result is preliminary, we expect that more sophisticated analysis will lead to a similar bound.

We can also examine the evolution of the globular cluster system from presumed initial conditions using eq. (13). As in the tidal case, we remark that the evolutionary sequences computed here only include the effects of black hole perturbations, not the better established effects known to operate, such as evaporation and disk shocking. For illustrative purposes, we adopted $N(M, 0) \propto M^{-2}$ for $10^3 M_\odot \leq M \leq 10^7 M_\odot$ (e.g. McLaughlin 1999). The results are shown in Fig. 9c,d. As can be seen, $N(M, t)$ evolves to a form reminiscent of today's cluster mass distribution over a time span $\Gamma_d t \sim 10$, which corresponds to ≈ 10 Gyr for $f_{bh} \approx 1.1(R/16 \text{ kpc})$. However, it is also clear from this figure, and from Fig. 9a,b, that the shape of $N(M, t)$ evolves somewhat more rapidly, on a timespan $\Gamma_d \Delta t \sim 2$ or 3, so the observed distribution is not long-lived. We note that the total mass in clusters drops by about a factor of ten between $\Gamma_d t = 0$ and $\Gamma_d t = 10$ for this model, which, although substantial, does not violate any observational constraints (cf. Klessen & Burkert 1996).

From these preliminary investigations, we conclude that while it is possible to find initial conditions $N(M, 0)$ that evolve to the observed distribution of cluster masses in ~ 10 Gyr even for $f_{bh} \sim 1$, the evolutionary timescale is rather short, so the distribution is rather unstable. Although a more precise treatment of the bounds on f_{bh} that can be derived from requiring stability of the cluster mass distribution needs to be done (and will be presented by us elsewhere), we are confident that the observed distribution is unstable unless $\Gamma_d t = N_d \lesssim 3$ everywhere in the halo. Adopting this rather conservative limit, we conclude provisionally that stability of the cluster mass function requires $f_{bh} \lesssim 0.34(R/16 \text{ kpc})$.

We therefore propose two different bounds on f_{bh} . The less restrictive of the two is the stability bound derived above. For direct comparison with the disk heating bound, we shall rescale all constraints to $R = 8$ kpc; then stability implies $f_{bh} \lesssim 0.17(R/8 \text{ kpc})$. This bound applies, strictly speaking, to $M_{bh} = 2 \times 10^6 M_\odot$. At much larger black hole masses, where the tidal approximation is valid, we found a similar bound based on mass loss from clusters to the halo, and we adopt $f_{bh} \lesssim 0.17(R/8 \text{ kpc})$ for all $M_{bh} \gtrsim 2 \times 10^6 M_\odot$. The more restrictive bound is obtained by assuming that a hypothetical cluster with $M_c = 2.5 \times 10^4 M_\odot$ on a circular orbit at 16 kpc should have no worse than a 50% chance of survival. Using the scalings given above to compute bounds at $R = 8$ kpc, we find $f_{bh} \lesssim 0.025$ for $f_d = 0.15$ and $f_{bh} \lesssim 0.05$ for $f_d = 0.5$. If we keep $M_c = 2.5 \times 10^4 M_\odot$ fixed, then these limits apply to $M_{bh} \gtrsim 1 \times 10^6 M_\odot$ and $M_{bh} \gtrsim 2 \times 10^6 M_\odot$, respectively. Since the evaporation time falls to about 10 Gyr

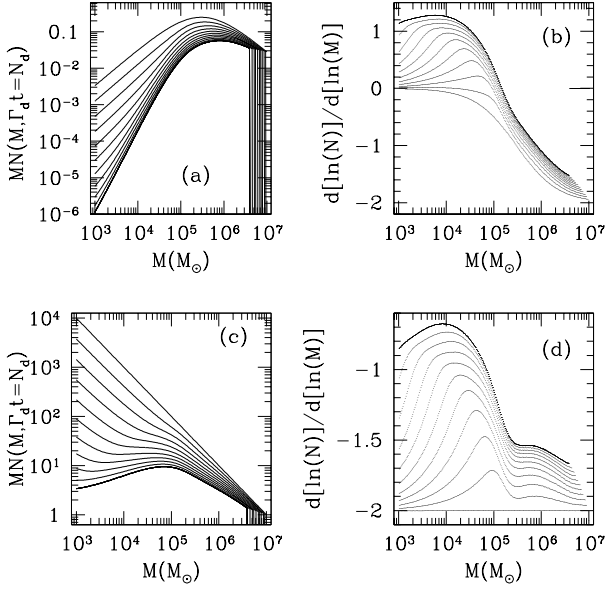


Figure 9. Panels (a-d) show the cluster population mass function and its power law index for a range of times. The initial condition $N(m, 0) = (1 + M/M_0)^{-2}/M_0$ was used in figures (a) and (b), and the initial condition $N(m, 0) = 1/M^2$ was used in figures (c) and (d). The eleven curves in each figure correspond to the times $\Gamma_d t = N_d = 0, 1, \dots, 10$. In figures (a) and (c), time increases as the curves go from top to bottom, while in figures (b) and (d) the opposite is true. The sharp edges seen at large masses occur where the mass function is zero in the advection/destruction model.

at $R = 8$ kpc for $M_c = 2.5 \times 10^4 M_\odot$ and $f_{bh} = 0$, we might prefer to keep the evaporation timescale fixed at 20 Gyr, in which case our derived limits on f_{bh} apply to slightly larger black hole masses, $M_{bh} \gtrsim 2 \times 10^6 M_\odot$ and $M_{bh} \gtrsim 3 \times 10^6 M_\odot$ for $f_d = 0.15$ and $f_d = 0.5$, respectively. For our conservative bounds, we adopt $f_{bh} \lesssim 0.05$ for $M_{bh} \gtrsim 3 \times 10^6 M_\odot$; for our most stringent bounds, we adopt $f_{bh} \lesssim 0.025$ for $M_{bh} \gtrsim 1 \times 10^6 M_\odot$. Figure 10 shows these limits along with the upper limit

$$M_{bh} < 4.4 \times 10^7 M_\odot \left(\frac{8}{\ln \Lambda} \right) \left(\frac{R}{8 \text{ kpc}} \right)^2, \quad (15)$$

for $\ln \Lambda = 8$ imposed by requiring that dynamical friction be incapable of dragging black holes inward in 10 Gyr (see equation [7-27] in Binney & Tremaine 1987), and the disk heating constraint $f_{bh} M_{bh} \lesssim 2 \times 10^6 M_\odot$ (Lacey & Ostriker 1985). The figure shows that the globular cluster constraint forbids considerable portions of $M_{bh} - f_{bh}$ space allowed by disk heating.

5 ACKNOWLEDGEMENTS

We would like to thank Scott Tremaine and the referee, Oleg Gnedin, for detailed discussion and many helpful comments. This work was supported by the Fund for Astrophysical Research and NASA NAG 5-3097.

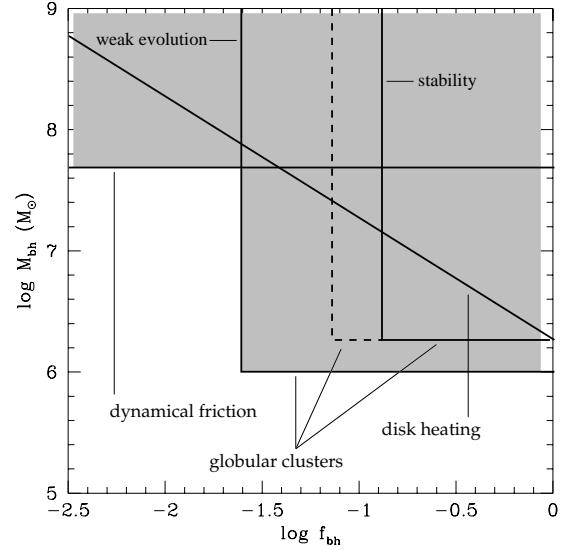


Figure 10. The constraints on the mass and fraction of black holes at 8 kpc in the halo. The solid horizontal line shows the upper limit on $\log M_{bh}$ from dynamical friction. For $\log M_{bh} \gtrsim 7.7$, black holes spiral into the Galactic center. The solid diagonal line shows the disk heating constraint: $\log f_{bh} M_{bh} \gtrsim 6.3$ overheats the disk. The solid box labeled *stability* shows the constraint obtained from the stability requirement for the globular cluster population, $\log f_{bh} < -0.77$ for $\log M_{bh} \gtrsim 6.3$. The dashed box shows the more conservative constraint for the weak cluster evolution hypothesis $\log f_{bh} \lesssim -1.3$ for $\log M_{bh} \gtrsim 6.3$ and the solid box labeled *weak evolution* shows the most stringent bound, $\log f_{bh} < -1.6$ for $\log M_{bh} \gtrsim 6$. The shading indicates regions which are disfavored by the combination of constraints.

APPENDIX A: SECOND-ORDER CHANGE IN DF IN IMPULSIVE ENCOUNTER

We derive the second-order change in the cluster DF due to an impulsive, tidal encounter with a perturber. As mentioned above, the resulting expression is equivalent to a Fokker-Planck equation for the change in the DF and therefore consists of an advection term and a diffusion term. Our derivation reveals an error in previous treatments (Kundic & Ostriker 1995; Gnedin & Ostriker 1997; Murali & Weinberg 1997a) which results from improper integration over velocity coordinates in projecting the advection and diffusion coefficients to energy space. As shown in the derivation and discussion below, the problem arises because one cannot integrate over the entire range of angular coordinates in velocity space: failure to restrict the integration domain corresponds to including fictitious transitions to bound states from unbound states that are, in reality, unoccupied initially. Mathematically, there is a θ -function implicit in the kinetic equation which has previously been ignored.

For any impulsive encounter with a perturber, the equation,

$$\begin{aligned} f_{new}(\mathbf{r}', \mathbf{v}') &= \int d\mathbf{r} d\mathbf{v} \delta(\mathbf{r} - \mathbf{r}') \delta(\mathbf{v} - \mathbf{v}' + \Delta\mathbf{v}(\mathbf{r})) f(\mathbf{r}, \mathbf{v}) \\ &= f(\mathbf{r}', \mathbf{v}' - \Delta\mathbf{v}(\mathbf{r}')); \end{aligned} \quad (A1)$$

gives an exact expression for the new DF, f_{new} , in terms of the old DF f . The δ -function in time indicates that the perturbation is impulsive; the δ -function in position indicates that particles do not move during the perturbation; and the δ -function in velocity defines the position-dependent velocity impulse (with respect to center of mass), $\Delta\mathbf{v}(\mathbf{r})$, imparted to a particle by the perturbation. Consequently, the new DF is the old DF with velocity bins shifted according to the position-dependent velocity impulse.

The resulting mass loss

$$\delta M = \int_{|\mathbf{v}'| > v_e(r')} d\mathbf{r}' d\mathbf{v}' f_{new}(\mathbf{r}', \mathbf{v}'), \quad (\text{A2})$$

is the integral over all particles whose new velocity is greater than the escape velocity $v_e(r)$. Substituting equation (A1) for f_{new} , we can show that

$$\delta M = \int d\mathbf{r} \int d\mathbf{v} \Theta(|\mathbf{v} + \Delta\mathbf{v}(\mathbf{r})| - v_e(r)) f(r, v), \quad (\text{A3})$$

where we have dropped the primes on the spatial coordinates. This is precisely equation (39) of Chernoff, Kochanek & Shapiro (1987) (hereafter CKS); therefore the present treatment of individual collisions is equivalent to that used by Arras & Wasserman (1998).

To use a one-dimensional, phase-space method like the standard Fokker-Planck calculation, we must project the new DF into energy space by integrating over all other coordinates. The projection

$$16\pi^2 P(E) f_{new}(E) \equiv \int d\mathbf{r} d\Omega_v \sqrt{2(E - \Phi)} f_{new}(\mathbf{r}, \mathbf{v}) = \int_{|\mathbf{v} - \Delta\mathbf{v}| < v_e(r)} d\mathbf{r} d\Omega_v \sqrt{2(E - \Phi)} f(\mathbf{r}, \mathbf{v} - \Delta\mathbf{v}(\mathbf{r})) \quad (\text{A4})$$

where the phase-space volume

$$P(E) = \int dr r^2 \sqrt{2[E - \Phi(r)]}. \quad (\text{A5})$$

The second integral in equation (A4) has a limited range of integration because the perturbation can transport unoccupied, unbound states to bound states: areas where the unperturbed DF vanishes, i.e. $E > E_t$, define the excluded regions. To reiterate, previous treatments have overlooked this subtlety in deriving the kinetic equation, thereby obtaining a factor of 2 overestimate in the mass loss.

To derive the second-order change, we expand f_{new} in a Taylor series about the unperturbed DF:

$$f_{new}(\mathbf{r}, \mathbf{v}) = f(\mathbf{r}, \mathbf{v} - \Delta\mathbf{v}(\mathbf{r})) \approx f(\mathbf{r}, \mathbf{v}) - \frac{\partial f}{\partial \mathbf{v}} \cdot \Delta\mathbf{v}(\mathbf{r}) + \frac{1}{2} \Delta\mathbf{v}(\mathbf{r}) \cdot \frac{\partial^2 f}{\partial \mathbf{v} \partial \mathbf{v}} \cdot \Delta\mathbf{v}(\mathbf{r}). \quad (\text{A6})$$

This has the standard form of the velocity-space Fokker-Planck equation. Substitution into equation (A4) yields an equation for the change in the DF, δf .

We will now briefly outline the calculation of δf . Let the direction of the relative velocity be along the z -axis and the position of a star in the cluster given by spherical radius r and the cosine of the angle with respect to the z axis, $\mu = \cos\theta$. The magnitude of the tidal velocity kick with respect to the center of mass of the cluster is then [see,

e.g., Arras & Wasserman (1998)]

$$\Delta v(\mathbf{r}) = \frac{2GM_{bh} r \sqrt{1 - \mu^2}}{b^2 V_{rel}}. \quad (\text{A7})$$

The region of phase space for which $|\mathbf{v} - \Delta\mathbf{v}| < v_e(r)$ has been discussed in both CKS and Arras & Wasserman (1998). They find that, depending on the energy E and the position r and μ , the velocity angle cosine $\mu_v = \mathbf{v} \cdot \Delta\mathbf{v} / v \Delta v$ may only extend over a restricted interval instead of $(-1, 1)$. Hence, spherical symmetry is broken and the first order term in Δv in equation A6 no longer integrates to zero. The end result is that there will be two different mathematical forms for δf depending on the energy E . Define the critical energy

$$E_{crit} = E_{max} - \frac{2GM_{bh} r_{peak}}{b^2 V_{rel}} v_e(r_{peak}) \quad (\text{A8})$$

where r_{peak} is the radius at which $r v_e(r)$ reaches a maximum. For energies $E < E_{crit}$, the velocity cosine μ_v is in $(-1, 1)$ for all values of r and μ and one would obtain the ‘‘standard’’ results for δf . For $E > E_{crit}$, on the other hand, μ_v runs over a restricted range and a different mathematical expression for δf is obtained.

It is convenient to write δf in the quasilinear form

$$\delta f(E) = [16\pi^2 P(E)]^{-1} \frac{dF(E)}{dE}. \quad (\text{A9})$$

For energies $E < E_{crit}$, we find

$$F(E) = \frac{64\pi^2}{9} \frac{df(E)}{dE} \left(\frac{GM_{bh}}{b^2 V_{rel}} \right)^2 \times \int_0^{\phi^{-1}(E)} dr r^4 (2[E - \phi(r)])^{3/2}, \quad (\text{A10})$$

where $\phi^{-1}(E)$ is the apocenter of a radial orbit with energy E . For $E > E_{crit}$, a more complicated expression results, given by

$$F(E) = + \frac{64\pi^2}{9} \frac{df(E_{max})}{dE} \left(\frac{GM_{bh}}{b^2 V_{rel}} \right)^2 \int_0^{r_t} dr r^4 v_e^3(r) - 8\pi^2 \frac{df(E_{max})}{dE} \int_{r_{min}(E)}^{r_{max}(E)} dr r^2 v_e(r) \times \left[+ \frac{1}{2} (E_{max} - E)^2 \mu_0(r, E) - \frac{1}{4} \frac{2GM_{bh} r}{b^2 V_{rel}} (E_{max} - E) \left\{ \frac{\pi}{2} - \theta_0(r, E) + \frac{1}{2} \sin(2\theta_0(r, E)) \right\} - \frac{1}{6} \frac{1}{v_e(r)} \frac{b^2 V_{rel}}{2GM_{bh} r} (E_{max} - E)^3 \left(\frac{\pi}{2} - \theta_0(r, E) \right) + \frac{1}{6} v_e^2(r) \left(\frac{2GM_{bh} r}{b^2 V_{rel}} \right)^2 \left\{ \mu_0(r, E) - \frac{1}{3} \mu_0^3(r, E) \right\} \right]. \quad (\text{A11})$$

Here $E = v^2/2 + \phi(r)$ is the energy (per unit mass), $E_{max} = \phi(r_t)$ and $E_{min} = \phi(0)$, r_t is the tidal radius of the cluster, f is the pre-collision distribution function, r_{max} and r_{min} are defined by the equation

$$\frac{b^2 V_{rel}}{2GM_{bh}} (E_{max} - E) = v_e(r_{min, max}) r_{min, max}, \quad (\text{A12})$$

and the cosine $\mu_0(r, E) = \cos(\theta_0(r, E))$ is defined by the equation

$$(1 - \mu_0^2(r, E))^{1/2} = \frac{b^2 V_{rel}}{2GM_{bh} r} \frac{1}{v_e(r)} (E_{max} - E). \quad (\text{A13})$$

For most of the range of E , the above equation gives the same result as if there were no restrictions on phase space. Only for energies within roughly $\Delta v/v$ of E_{max} do the restrictions make a difference. However, the flux at the boundary, which is the change in the mass of the cluster is significantly altered; we find

$$F(E_{max}) = \Delta M = \frac{32\pi^2}{9} \frac{df(E_{max})}{dE} \left(\frac{GM_{bh}}{b^2 V_{rel}} \right)^2 \int_0^{r_t} dr r^4 v_e^3(r). \quad (A14)$$

This is exactly a factor of two smaller than the answer obtained from ignoring the phase space restrictions.

For reference, we give the value of K used in equation (2):

$$K = \frac{32\pi^2}{9} G^2 \frac{1}{M} \left| \frac{df(E_{max})}{dE} \right| \int_0^{r_t} dr r^4 v_e^3(r). \quad (A15)$$

The above procedure is inherently linear and, therefore, has only a limited range of validity. The method fails because the new DF, $f_0 + \Delta f$, becomes negative as we increase the mass loss. We find that negative excursions in the new DF become unacceptably large for $dM/M \gtrsim 0.15$.

REFERENCES

- Alcock, C., Allsman, R. A., Alves, D., Axelrod, T. S., Becker, A. C., Bennett, D. P., Cook, K. H., Freeman, K. C., Griest, K., Guern, J., Lehner, M. J., Marshall, S. L., Peterson, B. A., Pratt, M. R., Quinn, P. J., Rodgers, A. W., Stubbs, C. W., Sutherland, W., Welch, D. L., The MACHO Collaboration, 1997, *ApJ*, 486, 697
- Arras, P., Murali, C. & Wasserman, I. 1999, *Constraints on the mass and abundance of black holes in the Galactic halo: the low-mass limit*, in preparation
- Arras, P. & Wasserman, I. 1998, *MNRAS*, in press (astro-ph/9811370)
- Ashman, K. & Zepf, S. 1998, *Globular Cluster Systems* (Cambridge: Cambridge University Press)
- Bahcall, J., Hut, P. & Tremaine, S. 1985, *ApJ*, 290, 15
- Beers, T. & Sommer-Larsen, J. 1995, *ApJS*, 96, 175
- Binney, J. & Tremaine, S. 1987, *Galactic Dynamics* (Princeton: Princeton University Press)
- Canizares, C. 1982, *ApJ*, 263, 508
- Carlberg, R., Dawson, P., Hsu, T. & van den Bergh, 1985, *ApJ*, 294, 674
- Carr, B. 1994, *ARA&A*, 32, 531
- Carr, B., Bond, J. R. & Arnett, D. 1984, *ApJ*, 277, 445
- Chernoff, D. & Weinberg, M. D. 1990, 351, 121
- Chernoff, D., Kochanek, C. & Shapiro, S. 1987, *ApJ*, 309, 183
- Drukier, G., Fahlman, G. & Richer, H. 1992, *ApJ*, 386, 106
- Gnedin, O. 1997, *ApJ*, 487, 663
- Gnedin, O. & Ostriker, J. 1997, *ApJ*, 487, 667
- Gomez, A., Delhaye, J., Grenier, S., Jaschek, C., Arenou, F. & Jaschek, M. 1990, *A&A*, 236, 95
- Harris, W. 1991, *ARA&A*, 29, 543
- Harris, W., Harris, G. & McLaughlin, D. 1998, *AJ*, 115, 1801
- Hut, P. & Rees, M. 1992, *MNRAS*, 259, 27
- Kassiola, A., Kovner, I. & Blandford R. 1991, *ApJ*, 381, 6
- Klessen, R. & Burkert, A. 1995, *MNRAS*, 280, 735
- Kormendy, J. & Richstone, D. 1995, *ARA&A*, 33, 581
- Kundic, T. & Ostriker, J. 1995, *ApJ*, 438, 702
- Kundu, A., Whitmore, B., Sparks, W., Macchetto, F., Zepf, S. & Ashman, K. 1998, *ApJ*, in press (astro-ph/9812199)
- Lacey, C. 1991, in *Dynamics of Disc Galaxies*, Sundelius, B. ed. (Goteborg), 257
- Lacey, C. & Ostriker, J. 1985, *ApJ*, 299, 633
- Lee, H., Fahlman, G. & Richer, H. 1991, *ApJ*, 366, 455
- McLaughlin, D. 1999, *AJ*, 117, 2398
- Moore, B. 1993, *ApJ*, 413, L93
- Murali, C. & Weinberg, M. D. 1997a, 291, 717
- Murali, C. & Weinberg, M. D. 1997b, 288, 767
- Murali, C. & Weinberg, M. D. 1997c, 288, 749
- Pagal, B. E. J. 1997, *Nucleosynthesis and chemical evolution of galaxies* (Cambridge : Cambridge University Press)
- Sellwood, J., Nelson, R. W. & Tremaine, S. 1998, *ApJ*, 506, 590
- Stromgren, B. 1987, in *Proceedings of the NATO ASI, The Galaxy*, Gilmore, G. & Carswell, B., eds. (Cambridge: Reidel), 229
- Turner, E. and Umemura, M. 1997, *ApJ*, 483, 603
- Turner, E., Wardle, M. & Schneider, D. 1990, *AJ*, 100, 146
- Vesperini, E. 1997, *MNRAS*, 287, 915
- Wasserman, I. & Salpeter, E. 1994, *ApJ*, 433, 670
- Wielen, R. 1988, in *IAU 126, The Harlow-Shapley Symposium on Globular Cluster Systems in Galaxies*, Grindlay, J. & Hut, P., eds. (Dordrecht:Kluwer), 393
- Wielen, R. 1985, in *IAU 113, Dynamics of Star Clusters*, Goodman, J. & Hut, P., eds. (Dordrecht:Reidel), 449
- Wielen, R. 1977, *A&A*, 60, 263
- Xu, G. & Ostriker, J. 1994, *ApJ*, 437, 184